Handbook of Sustainable Development through Green Engineering and Technology

Vikram Bali, Rajni Mohana, Ahmed A. Elngar, Sunil Kumar Chawla, Gurpreet Singh

Clay and Ceramics as Sustainable and Green Materials to Remove Methylene Blue from Water: A Critical Analysis

Publication details
https://test.routledgehandbooks.com/doi/10.1201/9781003127819-13
Priyanka Sharma, Kushal Qanungo
Published online on: 27 Sep 2022

How to cite :- Priyanka Sharma, Kushal Qanungo. 27 Sep 2022, *Clay and Ceramics as Sustainable and Green Materials to Remove Methylene Blue from Water: A Critical Analysis from:* Handbook of Sustainable Development through Green Engineering and Technology CRC Press
Accessed on: 28 May 2023
https://test.routledgehandbooks.com/doi/10.1201/9781003127819-13

13 Clay and Ceramics as Sustainable and Green Materials to Remove Methylene Blue from Water: A Critical Analysis

Priyanka Sharma and Kushal Qanungo
Division of Chemistry, University Institute of Science, Chandigarh University, Gharuan, Mohali, Punjab, India

CONTENTS

13.1 INTRODUCTION

Water pollution is a global phenomenon, and it adversely affects both biotic and abiotic components of the ecosystem. Furthermore, rapid industrialisation has

DOI: 10.1201/9781003127819-13

resulted in the production of different organic and inorganic pollutants that pollute the surface and groundwater, making it unsuitable for agricultural, industrial, and domestic use (Noel & Rajan, 2015; Shahadat & Isamil, 2018).

The dyeing industry is one of the heavily polluting industries. Due to the water-soluble nature of the most dyes and their high molar-extinction coefficient, they are visible, even at a very low concentration. Effluents generated from dyeing industries contain a considerable volume of dye-containing wastewater (Reisch, 1996). Due to their synthetic origin and the thermal and photo-stable nature of most dyes, they are nonbiodegradable and can exist in the environment for a long time (Ho & Chiang, 2001; Bhatia et al., 2017). These dye effluents contain many chemicals that are lethal, carcinogenic, and mutagenic to living organisms. Therefore, treatment or removal of these harmful pollutants is essential before discharging the wastewater into the environment, and thus, wastewater treatment is a great challenge for scientists and environmental engineers.

Dyes are chemicals that are used to colour different substances like paper, rubber, plastics, cosmetics, leather and textiles. They have diverse chemical composition and structures. Methylene blue (MB) is a cationic azo dye ($C_{16}H_{18}ClN_3S$). It is a solid, odourless, dark-green powder at room temperature and gives blue colour on dissolving in water. MB is used for staining cells and tissues in microbiology and pathological laboratories (Vutskits et al., 2008). Furthermore, it is also used in pharmaceutical industries, paper industries, and to dye cotton, silk, and wool. However, it can cause many health issues, like irritation and paleness of the skin (necrosis), burning sensation, shortness of breath, inflammation, nausea, vomiting, weakness, and mental confusion (Bleicher et al., 2009).

13.1.1 Dye Separation Methods

Numerous methods are employed to remove harmful pollutants/dyes from aqueous systems. These methods include physical, chemical, and biological processes like oxidation, membrane filtration, coagulation, ion exchange, aerobic degradation, and adsorption, etc. (Mondal, 2008).

Among different dye-removal methods, adsorption is one of the most preferred low-cost and flexible methods due to its easy handling and efficient dye-removal power. Adsorption involves the movement of solute (ions, atoms, molecules) from the solution phase to the adsorbent surface. The adsorbate molecules can be liquid, gas, or solid (Kandisa et al., 2016).

The process of adsorption is generally of two types: physisorption and chemisorption. In the process of physisorption or physical adsorption, the molecules of adsorbate adsorb on the surface of the adsorbent through forces like ionic interactions, hydrogen bonding, van der Waals forces, etc. Physical adsorption is generally an efficient method since it requires low activation energy; also, multilayered adsorption is possible in many cases. On the other hand, chemisorption/chemical adsorption is a process that involves the exchange of electron/ion/chemical-bond formation during adsorption (Dawood & Sen, 2014).

13.1.2 Clay and Ceramic Materials as Adsorbent

Clays are emerging as an alternative adsorbent for pollutants removal from wastewater because of their low cost, natural abundance, inorganic and ecofriendly nature (Santos et al., 2016).

Clays are hydrated aluminosilicates with a variable amount of other ions, such as Mg, Fe, alkali, and alkaline earth metals, with a particle size of less than 2 μm. Kaolinite, montmorillonite-smectite, illite, and chlorite are the major groups of clays. The kaolinite group includes kaolinite, dickite, halloysite, and nacrite minerals. The minerals pyrophyllite, talc, vermiculite, sauconite, saponite, nontronite, and montmorillonite, are present in the smectite group. Clay micas are in illite group (Adeyemo et al., 2017). Clay has several advantages, including high specific surface area, ion-exchange potential, good adsorption power, and nontoxic nature. However, very few reports show ceramics being used as an adsorbent material for MB removal (Njoya et al., 2017).

This chapter aims to give a comprehensive study of the use of clay and ceramics materials in their raw or modified forms as an adsorbent for MB removal. Different types of clays from around the world, either in natural or modified form, have been used in MB removal and have been critically analysed and discussed. These clays include: Saudi red clay (SC), natural illite clay mineral (NICM), raw bentonite (RB), plasma-modified bentonite clay (PMBC), Moroccan clay (MC), montmorillonite clay (MIC), raw ball clay beads (RBCB), modified ball clay beads (MBCB), mesoporous synthetic hectorite clay (MSHC), modified Tamazert kaolin (KT), fibrous clay mineral (FCM), calcined kamerotar clays (CKC), silonijan kaolin (SK), calcined natural clay (CNC), natural clay material (NCM), erzurum clay (EC), topkhana natural clay (TNC), modified ball clay (MBC), modified ball clay-chitosan composite (MBC-CH), and many other clay-ceramic based adsorbents. Furthermore, the adsorption behaviour of clays and ceramics has also been analysed by comparing different experimental conditions, like adsorption capacity, concentration, temperature, adsorbent dose, pH of the solution, presence of co-ions, adsorption mechanism, and kinetics involved during adsorand mental confusionption of MB molecules.

13.2 MATHEMATICAL EQUATIONS

13.2.1 Calculation of Adsorption Capacity and Removal Percentage

The amount of dye adsorbed ($mg.g^{-1}$) and removal percentage (%) can be calculated using the following equation (Suteu & Malutan, 2013; Arora et al., 2019).

$$q_t = \frac{Co - Ce}{w} V$$

$$\text{Removal } \% = \frac{(C_o - C_e)}{C_o} \times 100$$

Where w is the mass of adsorbent used and V is the volume of the solution.

13.2.2 Kinetics Models Used for Adsorption Analysis

Model	Mathematical Equation	Plot	Parameters	References
Pseudo first order (PFO)	Linear: $\ln(q_e - q_t) = \ln q_e - K_1 t$ Non-linear: $q_t = q_e(1 - e^{-K_1 t})$	$\ln(q_e - q_t)$ *vs* t	q_t = amount of dye adsorbed at time q_e = amount of dye adsorbed at equilibrium t = Contact time K_1 = Pseudo-first-order rate constant. K_2 = Pseudo-second-order rate constant	(Moussout et al., 2018)
Pseudo second-order (PSO)	Linear: $\frac{t}{q_t} = \frac{1}{k_2 q_e^2} + \frac{t}{q_e}$ Non-linear: $qt = \frac{q_e^2 K_2 t}{q_e K_2 t + 1}$	t/q_t *vs* t		
Intraparticle diffusion	$q_t = K_{id}\, t^{0.5}$	q_t *vs* $t^{0.5}$	q_t = Amount of dye adsorbed at time t. K_{id} = Intraparticle diffusion rate constant.	(Doğan & Alkan, 2003)

13.2.3 Adsorption Isotherm Models Used for Analysis

Model	Mathematical Equation	Plot	Parameters	References
Langmuir	Nonlinear: $q_e = \frac{q_{max}\, bC_e}{1 + bC_e}$ Linear: $\frac{C_e}{q_e} = \left(\frac{C_e}{q_m}\right) + \left(\frac{1}{b \cdot q_{max}}\right)$ Separation factor: $R_L = \frac{1}{1 + bC_o}$	q_e *vs* C_e $\frac{C_e}{q_e}$ *vs* C_e	q_{max} = maximum Langmuir uptake Ce = equilibrium dye concentration *b* = Langmuir adsorption equilibrium constant R_L = Separation factor $R_L > 1$: Unfavourable $R_L = 1$: Linear $0 < R_L < 1$: Favourable $R_L = 0$: Irreversible	(Chen, 2015)
Freundlich	Nonlinear: $\log q_e = \log K_F + \frac{1}{n} \log C_e$ Linear (when n = 1): $q_e = K_F C_e^{1/n}$	$\log q_e$ *vs* $\log C_e$	K_F = Freundlich constants 1/n = Sorption intensity	(Wang & Guo, 2020)
Henry	$q_e = K_H C_e$	q_e *vs* C_e	K_H = Henry's adsorption binding constant	(Nnenna et al., 2020)

13.3 EXPERIMENTAL FACTORS IN MB REMOVAL

13.3.1 Effect of Contact Time

The reaction time plays a critical role in the course of adsorption. Commonly, the quantity of dye adsorbed ($mg.g^{-1}$) increases with the passage of time, which indicates filling of available adsorption sites during the initial reaction period.

Clay material, like SC, NICM, PMBC, MC and cordite-based ceramics (CBC), showed maximum removal within a time range of 5 to 60 min, whereas some adsorbents, like EC, MIC, MBCB, RBCB, KT, FCM, SK, CKC, MBC, and MBC-CH, took more time (60 to 180 min) to adsorb MB from the solution phase. The use of CKC showed a time of 20 h to absorb MB and to achieve the equilibrium stage.

The adsorption of MB using EC (rich in montmorillonite and nontronite) reached equilibrium at 60 min showed a maximum adsorption capacity of 58.2 $mg.g^{-1}$ (Gurses et al., 2006). For SC, the adsorption process was fast for the initial 5 min, and it took 40 min to reach adsorption equilibrium at a stirring rate of 150 rpm. There was a very steady rise in dye adsorption after the first 5 min, which is attributed to the negatively charged adsorbent surface, responsible for rapid electrostatic adsorption of MB at neutral pH of the solution (Khan, 2020). The CBCs with a variable composition of kaolinite, talc, and bauxite at different time intervals (0–30 min) also showed maximum adsorption for the first 5 min for different ceramic samples prepared by heating at 1300°C, 1400°C temperature (Njoya et al., 2017). MC showed promising results with a maximum adsorption rate in the first 5 min and reached equilibrium in 15 min, which indicates a fast movement of MB molecules on the surface of clay particles during initial reaction time and then the movement of dye molecules from the external surface to interlaminar regions. In contrast, kaolin took 7 h to reach equilibrium with 75% removal of MB from solution (El Mouzdahir et al., 2007). On using MIC for MB removal, equilibrium was achieved in less than 30 min, (Almeida et al., 2009).

Comparable results were also observed for MB adsorption experiments with polyamide-vermiculite nanocomposite (PVNC) with a 99% removal within a time range of 15 to 60 min with 15 $mg.L^{-1}$ of PVNC (Basaleh et al., 2019). For Algerian palygorskite (AP), 97% of removal was observed after a contact time of 5 min with a clay mass (50 $mg.L^{-1}$) with a MB concentration of 10 ppm (Youcef et al., 2019).

13.3.2 Effect of Solution pH

Several studies have suggested that the pH of a solution is one of the major factors that control the removal capacity and the adsorption efficiency of any adsorbent during the whole adsorption process. The change in pH of the solution can change the surface characteristics of the adsorbent as well as ionisation of dye molecules. It can alter the magnitude of dissociation of different functional groups present on the available active sites of the adsorbents. Basic pH in cationic dyes commonly results in a higher removal percentage due to the presence of the negatively charged surface (Khenifi et al., 2007; Nandi et al., 2009; Karaca et al., 2013). Most of the MB adsorption studies have been carried out in a pH range of 2–12. Furthermore,

the regeneration capacity of an adsorbent is influenced by the changes in pH of the regenerator solution. Commonly used reagents for altering or changing the concentration of H^+ and OH^- ions for regeneration of adsorbents are HCl and NaOH.

An increased adsorption capacity of mesoporous synthetic hectorite-alginate-beads (MSHC-AB) was found on raising the pH 3 to 10, and the highest removal (97.5%) was observed at a pH range of 12 (Pawar et al., 2018). A similar trend was also observed during MB adsorption using MIC, where both the adsorption capacity and the removal percentage were observed to be more at a basic pH range. This is ascribed to the increase in negative charge on the exterior sides of the adsorbent. MB removal using KT under basic conditions showed maximum adsorption (111 $mg.g^{-1}$) at a pH of 11.2, indicating a more negatively charged surface. In contrast, the lower adsorption (96 $mg.g^{-1}$) was observed in a pH range between 2.6 and 4.8, indicating the presence of a more positive charge on the surface of the adsorbent (BouKhemakhem & Rida, 2017). In the case of CBC, MB removal was studied within a range of 6–12, and maximum adsorption was at a pH of 6 within a contact time of 10 min (Njoya et al., 2017).

Similarly, an increased rate of adsorption was observed when the pH of the solution was changed from 4 to 12 using MBC and MBC-CH; a reverse trend was observed on decreasing the pH value (Auta & Hameed, 2014). Adsorbents like MC, SC, and EC were used to study MB adsorption, and they showed maximum adsorption at a neutral pH range. MB adsorption using CKC showed maximum adsorption at a pH of 7, and after that, remained stable, up to a pH of 12 (Duwal et al., 2016). Change in the pH (from 2–9) does not affect the adsorption capacity of TNC. The result obtained for TNC showed that the maximum percentage variation in adsorption capacity was less than 0.9% for MB solutions having different pH (Salh et al., 2020). An increase in pH of the reaction mixture from 2 to 6 for Iraqi Red Kaolin Clay (IRKC) resulted in a rise in adsorption capacity from 79.2 $mg.g^{-1}$ to 88.3 $mg.g^{-1}$ with pH_{pzc} (pH at point of zero charge) of 7 (Jawad & Abdulhameed, 2020). A similar trend was observed for MB adsorption on PVNC when the pH was increased from 3 to 10 resulting in an increase in removal efficiency from 35% to 75%. In addition to the electrostatic forces between MB and clay surface, a strong competition between MB^+ and H^+ ions at lower pH values play an important role in MB adsorption on clay (Basaleh et al., 2019).

13.3.3 Effect of MB Concentration

The initial concentration of solution provides the driving force required to move the solute particles from solution to the adsorbent surface. RB, NICM, MIC, EC, and KT showed a rise in adsorption capacity with increased MB concentration in solution. It follows that the removal mechanism, as well as withholding of the MB molecules by the adsorbent, becomes more efficient with the increase in dye concentration. This kind of adsorbent behaviour has been ascribed to the involvement of chemisorption, multilayer adsorption, or dimerization of MB molecules at a higher concentration range. Similar results were also obtained for CBC, as well as for MC.

In the case of adsorbents like MSHC and NICM, adsorption was found to be more effective with increased MB concentration, but the removal percentage was found to

be decreased at higher solution concentrations. The dye uptake showed a decrease in removal capacity with the saturation of the available active sites at a higher concentration of MB (Almeida et al., 2009; Ozdes et al., 2014; Pawar et al., 2018).

For MBC-CH, a range of uptake capacity of 26.93 to 193.23 $mg.g^{-1}$ was obtained for a concentration range of 30 to 300 $mg.L^{-1}$. This increase in adsorption capacity is attributed to the presence of numerous active sites on MBC-CH surface, which can easily surpass the limited number of MB molecules at low concentrations. In contrast, at a higher concentration of MB, there is competition for active sites present on the surface (Auta & Hameed, 2014). The use of bentonite alginate beads (BAB) also showed an increased rate of adsorption with the rise in MB concentration, which is attributed to the rapid diffusion of dye molecules at higher concentration (Pandey, 2019). Adsorption of MB using TNC also showed an increase in adsorption capacity from 25 $mg.g^{-1}$ to 128 $mg.g^{-1}$ on increasing MB concentration from 50 $mg.L^{-1}$ to 550 $mg.L^{-1}$ and this was accompanied by a decrease in adsorption power due to saturation of the sites of clay surface (Salh et al., 2020). Similarly, the use of IRKC showed a rise in adsorption capacity from 2.2 to 101.6 $mg.g^{-1}$ with a change in concentration from 10 to 120 $mg.L^{-1}$. The increased concentration gradient provides a driving force to transfer the MB molecules to active sites.

MB removal using MSHC and MSHC-AB composite showed a high MB removal efficiency with a low initial MB concentration (5–100 $mg.L^{-1}$), and it showed a slight decrease with a higher initial MB concentration of 5–800 $mg.L^{-1}$ (Pawar et al., 2018).

13.3.4 Effect of Adsorbent Dose

Usually, in the adsorption process, an increase in adsorbent dose results in an increase in removal efficiency. This is attributed to the rise in the number of existing adsorption sites at the adsorbent surface (Li et al., 2009; Saka & Sahin, 2011).

In the case of EC, an increased removal capacity (57.1 to 66.1 $mg.g^{-1}$) was obtained on varying the dose from 0.10 g to 0.30 g for a contact time of 120 min (Gurses et al., 2006). A variation in the dose of MC from 1.6 $g.L^{-1}$ to 4.6 $g.L^{-1}$ for MB concentration of 600 $mg.L^{-1}$ resulted in an increase in the MB removal percentage at the large dosage of adsorbent (Almeida et al., 2009). An increase in MB percentage removal from 66% to 100% was observed in response to an increase in the dose of KT clay from 1 $g.L^{-1}$ to 1.8 $g.L^{-1}$ (El Mouzdahir et al., 2007). Similarly, for TNC, MB adsorption increased on increasing the dose from 1 $g.L^{-1}$ to 5 $g.L^{-1}$ (Basaleh et al., 2019), and the use of a dose of 3.4 $g.L^{-1}$ showed a 100% removal with an adsorption capacity of 165 $mg.g^{-1}$. A variation in dose from 0.02 g to 0.2 g per 100 mL at a constant solution pH (5.6) and concentration (100 $mg.L^{-1}$) for IRKC resulted in an increased removal percentage value, from 86.2% to 99.8%, which is ascribed to availability of more surface area/active sites (Jawad & Abdulhameed, 2020).

SC as an adsorbent showed MB adsorption capacity of 50.25 $mg.g^{-1}$ with a dose of 0.2 g in a MB solution of 50 mL. The clay showed a sharp rise in the adsorption power with a lower dose, whereas the increase in dosage showed a slight increase in the removal efficiency. It is attributed to the agglomeration of clay particles, leading

to a decrease in adsorption sites and, therefore, reduction in the amount of MB adsorbed per unit mass of adsorbent and strong competition among MB molecules for a specific number of adsorption sites (Khan, 2020). An increase in the amount of NICM from 1.0 $g.L^{-1}$ to 30.0 $g.L^{-1}$ resulted in an increase in removal percentage from 81.4% to 99.0%. This is attributed to the increased number of clay particles, which leads to easy penetration of MB molecules onto the active adsorption sites. On the other hand, an increase in amount of NICM resulted in decreased MB uptake from 81.4 $mg.g^{-1}$ to 3.3 $mg.g^{-1}$, due to the aggregation of clay particles, which results in reduction in surface area for adsorption (Ozdes et al., 2014).

Similarly, in the case of CBC, MB adsorption showed a decrease with an increase in the amount of adsorbent. It is ascribed to the agglomerations of particles at higher ceramic dose, which leads to reduced adsorption sites, leading to a decreased value of MB adsorbed per unit mass of ceramic (Njoya et al., 2017).

SK also showed a reduced value of MB adsorption with an increased adsorbent dose. This is because of a decrease in equilibrium dye concentration with an increase in the dosage of SK (Ghosh & Bhattacharyya, 2002). Similar results were also obtained for MB adsorption by FCM, which is ascribed to the micro-aggregation of fibres (Hajjaji et al., 2006).

13.3.5 Effect of Temperature

Temperature plays an essential role in the adsorption process as it provides information regarding the enthalpy and entropy changes involved during the adsorption. The rate of diffusion of solute molecules across the outer boundary, as well as in the interior pores of the adsorbent, is affected by the change in temperature. Additionally, a change in reaction temperature can alter the equilibrium adsorption capacity. The influence of temperature on the adsorption capacity of different clay and ceramic materials is discussed below.

Experimental data for adsorbents like NICM, FCM, and SK, showed that these adsorbents are excellent adsorbent for MB removal at room temperature (298K). MB removal percentage for SC was observed to increase on increasing the temperature from 25°C to 55°C (Khan, 2020).

MB removal experiment using EC under a range of reaction temperature, i.e. 20°C, 40°C and 60°C showed that the rise in temperature causes a decrease in both efficiency and effectiveness of the adsorption process.

Temperature variation (5°C–40°C) studied with NICM as an adsorbent at a constant adsorbent dose (5.0 $g.L^{-1}$) and concentration (100 $mg.L^{-1}$) resulted in a slight increase in adsorption capacity on the increase in temperature. The results have been ascribed to a decrease in viscosity of solution or increase in the mobility of dye molecules, resulting in easy diffusion of dye molecules throughout the external surface as well as in the internal pores of clay particles. The increase in adsorption capacity with increasing temperature also signifies the endothermic nature of the adsorption process (Ozdes et al., 2014).

A change in temperature from 35°C to 60°C for MIC resulted in an increase in removal percentage from 68% to 74%, as well as a rise in the amount of MB adsorbed from 245 $mg.g^{-1}$ to 300 $mg.g^{-1}$, respectively. This 6% increase in

removal percentage indicates the endothermic nature of the adsorption process (Almeida et al., 2009). Similarly, a variation in temperature from 30°C to 50°C for RBCB and MBCB showed that a rise in reaction temperature resulted in better dye adsorption, which has been attributed to more significant collisions between solute and solvent molecules resulting in high adsorption rate (Auta & Hameed, 2014). The MB adsorption using TK was more feasible at a higher temperature (291K, 303K, 323K), which indicates the endothermic nature of the process (BouKhemakhem and Rida, 2017).

13.3.6 Effect of Other Ions

Co-ions have a variable effect on the adsorption behaviour of the adsorbent. The presence of co-ions may result in screening of the electrostatic interaction between the active sites and the dye molecules. In addition, the presence of ionic species could also result in an increase in the dissociation of the dye molecules, which is brought about by protonation.

In the removal of MB by MSHC-AB, the adsorption capacity has followed the order; sulphite < chloride < phosphate < bicarbonate < nitrate (Pawar et al., 2018). Results obtained for MBC and MBC-CH showed that the ionic species like SO_4^{2-} had a greater effect on MB adsorption in MBC and MBC-CH than ions like HCO_3^- and Cl^- (Auta & Hameed, 2012).

The presence of ionic species like $NaNO_3$, Na_2SO_4, $CaCl_2$, and KCl had a variable effect on MB adsorption on NICM. A higher strength of Na_2SO_4 (0 to 1.0 M) in the solution resulted in a decrease in the MB adsorption capacity (16.4 to 16.1 $mg.g^{-1}$). On the other hand, increase in strength of $NaNO_3$, KCl, and $CaCl_2$ ions from 0 to 1.0 M, resulted in an increase in the adsorption capacity; a change in q_e value from 16.4 to 16.9 $mg.g^{-1}$ for $NaNO_3$, 16.4 to 18.6 $mg.g^{-1}$ KCl and 16.4 to 18.7 $mg.g^{-1}$ in case of $CaCl_2$, respectively (Ozdes et al., 2014)

13.3.7 Kinetics and Mechanism

The adsorption kinetics is an essential and noteworthy factor that helps in choosing and finalising the optimal operating conditions for adsorbent-adsorbate interaction. To understand the adsorbent behaviour and to explore the reaction controlling mechanism, models like PFO, PSO, and intraparticle diffusion are suitable and have been extensively used.

For RB, the adsorption process was well explained by the PSO kinetic model as compared to PFO (Özacar & Şengil, 2006). Similarly, experiment data obtained for MSHC, NICM, RBCB or MBCB, KT, PMBC, CBC, and MC was fitted in the PSO. Correlation coefficient (R^2) for most of the adsorbents using the PSO model were higher than that of the PFO kinetic model, indicating that the MB adsorption can be described more accurately by the PSO.

In the case of FCM as an adsorbent, the MB adsorption was found to be diffusion-controlled, and the kinetics followed was PSO.

The use of BAB showed PSO kinetics and intraparticle diffusion involvement during the adsorption of MB on beads (Pandey, 2019). The use of TNC also showed

PSO kinetics and the adsorption phenomena controlled by fast film diffusion on external sites of clay and a slower diffusion on the inner sites of TNC (Salh et al., 2020). MB adsorption by IRKC showed high R^2 values followed PFO (Jawad & Abdulhameed, 2020).

13.3.8 Adsorption Studies

The adsorption isotherms are one of the most essential characteristics of an adsorbent-adsorbate interaction. The amount of dye accumulated on the adsorbent is typically analysed using adsorption isotherm models. It is a constant-temperature equilibrium correlation between the number of dye molecules per unit mass of clay (q_e) and equilibrium dye concentration (C_e). Different adsorption isotherm models are available for proper understanding of the equilibrium adsorption process and to know the mechanism of the adsorption process.

For SC, monolayer adsorption on the surface is indicated by a high correlation coefficient for the Langmuir isotherm model. Furthermore, the positive value of entropy suggests the spontaneous, endothermic, physical nature of the adsorption process, as well as randomness at the adsorbent/adsorbate interface (Khan, 2020). In the case of Pendik Bentonite (PB), the monolayer saturation capacity, (q_e), 1667 $mg.g^{-1}$, suggested that MB adsorption is restricted to monolayer coverage and well followed by the Langmuir isotherm (Özacar & Şengil, 2006). A comparative study between mesoporous synthetic hectorite-alginate-beads-wet (MSHC-AB-W) and powdered MSHC has shown a higher Langmuir monolayer adsorption capacity (785.45 $mg.g^{-1}$) for MSHC-AB-W, which signifies the differences in porosity and the number of available active sites for the adsorption of MB (Pawar et al., 2018). MB adsorption using NICM is also well demonstrated using the Langmuir isotherm study. Furthermore, the favourable nature of the adsorption process is indicated by the value R_L (0.32–0.02) and 1/n (0.12) for a concentration range of 50 $mg.L^{-1}$ to 1000 $mg.L^{-1}$. The high value of adsorption energy (25.0 kJ $mol.L^{-1}$) indicates the chemical nature of adsorption process during adsorption of MB by NICM particles (Ozdes et al., 2014). Similarly, for KT, MB adsorption using Langmuir showed monolayer adsorption suggesting a homogeneous nature of the clay surface (BouKhemakhem & Rida, 2017). In case of FCM, the cation exchange process is found to be responsible for the fast diffusion of MB molecules, and it was well followed by Langmuir isotherm for a variable pH range (4–9) (Hajjaji et al., 2006). For adsorbents, MBC and MBC-CH, the adsorption process is also well followed by the Langmuir model. Comparative isotherm study for MBC and MBC-CH showed a higher value of monolayer coverage for MBC-CH than MBC (Auta &Hameed, 2014). A straight-line plot in the case of CBC and MC showed fitting of experimental data in Langmuir isotherm (Njoya et al., 2017) (El Mouzdahir et al., 2007). Langmuir and Freundlich models were well followed by MB adsorption on IRKC with a high R^2 value of 0.99 and 0.98, respectively, indicating monolayer and multilayer mode of adsorption (Jawad & Abdulhameed, 2020).

The different clay and ceramic materials used to remove MB from aqueous solutions and their associated experimental conditions are tabulated in Table 13.1.

TABLE 13.1
Comparison of Different Experimental Parameters/Result

Sl. No.	Substrate	Experimental Conditions						Results					References
		Surface Area (m^2/g^{-1})/ Particle Size	RPM	Time (min)	pH	Adsorbent Dose ($g.L^1$)	MB Conc. ($mg.L^{-1}$)	Ads. Cap. (q_e) Max. ($mg.g^{-1}$)	Removal (Max.) (%)	Kinetic Model	Rate Constant ($g.mg^{-1}.min^{-1}$)	Adsorption Model	
1	SC	63.15/-	150	60	7	0.1–0.7	100	50.25	100	PSO	0.552	Langmuir	(Khan, 2020)
2	PB	28/53–75 μm	500	60	7.9	1.0	100–1000	1667	978	PSO	13.09×10^{-4}	Langmuir	(Özacar & Şengil, 2006)
3	EC	30/-	90–200	15–120	5.65	0.10–0.30	10–100	58.2	–	PSO	0.00178	Langmuir	(Gurses et al., 2006)
4	MSHC	468/-	–	60–900	3–12	1–5	5–800	196	97.50	PSO	–	Langmuir	Pawar et al., 2018)
	MSHC-AB-D	205/-						357.14		PFO		Freundlich	
	MSHC-AB-W	205/-						485.45		PFO		Freundlich	
5	NICM	3.10/-	400	60	2–10	1–30	50–1000	24.87	92.3	PSO	0.045	Langmuir	Ozdes et al., 2014)
6	MIC	62/-	250	120	3–11	1.6–4.6	200–1500	300.30	100	PSO	456.82×10^{-2} ($g.mg^{-1}.h^{-1}$)	Langmuir	Almeida et al., 2009)
7	MBCB	92/1–2 mm	140	1440	3–12	0.20 g/ 200 mL	30–300	100	96	PSO	2.070×10^{-4} ($g.mg^{-1}.h^{-1}$)	Langmuir	(Auta & Hameed, 2012)
8	RBCB	10/1–2 mm						34.652	53		65.90×10^{-4} ($g.mg^{-1}.h^{-1}$)		
9	KT	14/-	400	5–120	2–11.19	1.0–6.0	30–100	111	66–100	PSO	0.0013–0.004	Langmuir	(BouKhemakhem and Rida, 2017)
10	RB	64.2/-	100	180	2–12	0.15 g/ 200 mL	100–250	303	–	PSO	0.00247–0.0568	Langmuir	(Sahin et al., 2015)
	PMBC	65.3/-											
11	FCM	115/<2 μm	10,000	100	4–9	0.3	10–25	85	–	diffu-sion	$(29 \pm 3) \times 10^{-3}$ min^{-1}	Langmuir	(Hajjaji et al., 2006)

(*Continued*)

TABLE.13.1 (Continued)
Comparison of Different Experimental Parameters/Result

Sl. No.	Substrate	Experimental Conditions						Results					References
		Surface Area (m^2/g^{-1})/ Particle Size	RPM	Time (min)	pH	Adsorbent Dose ($g.L^1$)	MB Conc. ($mg.L^{-1}$)	Ads. Cap. (q_e) Max. ($mg.g^{-1}$)	Removal (Max.) (%)	Kinetic Model	Rate Constant ($g.mg^{-1}.min^{-1}$)	Adsorption Model	
12	SK	–	–	180	2–10	0.8	10–25	20.49	–	Fick's law –	–	Langmuir	(Ghosh & Bhattacharyya, 2002)
13	CKC	-/<63 μm	–	10–140	7–12	100 mg/ 50 mL	25–55 m mol.L^{-1}	19.47 mmol.g^{-1}	–	–	–	Langmuir	(Duwal et al., 2016)
14	MBC	-/0.5–2.0 mm	–	100	4–12	0.10 g/ 100 mL	30–300	70	–	PSO	0.629–4.870 ($g.mg^{-1}.h^{-1}$)	Langmuir	(Auta & Hameed, 2014)
	MBC–CH							142					
17	CBC	–	–	5–35	6–12	0.1–0.5 g	5–11	1.84		PSO	1.897	Langmuir	(Njoya et al., 2017)
18	MC	414/-	350	5–15	7.2	0.1 g	10–1000	135	–	PSO	0.0050	Langmuir	(El Mouzdahir et al., 2007)
19	BAB	-/2.76 mm	160	30	7	0.05% (w/v)	200–1500	2024	85	PSO	1.92×10^{-4}	Langmuir	(Pandey, 2019)
20	TNC	-/<5 μm	5000	0–360	2–9	1–5	10–250	129.8	≈100	PSO	0.00209	Langmuir	(Salh et al., 2020)
21	IRKC	-/≤250 μm	110	0–300	8	0.10 g/ 100 mL	10–120	240.4	99.8	PSO	0.18	Langmuir	(Jawad & Abdulhameed, 2020)
22	PVNC	12.307/-	4400	180	3–10	5–50 mg	15	76.42	99	PSO	0.002375	Langmuir	(Basaleh et al., 2019)
23	AP	-/5–100 μm	–	5–60	–	50g	10	57.47	97	PSO	–	Langmuir	(Youcef et al., 2019)

24	Kaolin (Halloysite)	70.90/-	–	5–30	3–11	25 mg/ 25 mL	5–30	29.13	–	PSO	1.05–0.01	–	(Harrou et al., 2020)
	Kaolin (kaolinite)	6.19/-						26.47					
25	Ngbo Clay	-/0.75 µm	150	60	2–12	0.5–5 g/ 100 mL	100–900	–	97	PSO	377.69	Freundlich Henry	(Nnenna et al., 2020)
26	NCM	/75 µm	–	300	–	2 mg/40 mL	10–50	18.8–97.2	–	PSO	0.016	Freundlich	(Nyankson et al., 2020)
27	Pakistani Clay	–	–	10–380	2–10	–	50–300	270	–	PSO	–	Langmuir	(Rehman et al., 2021)

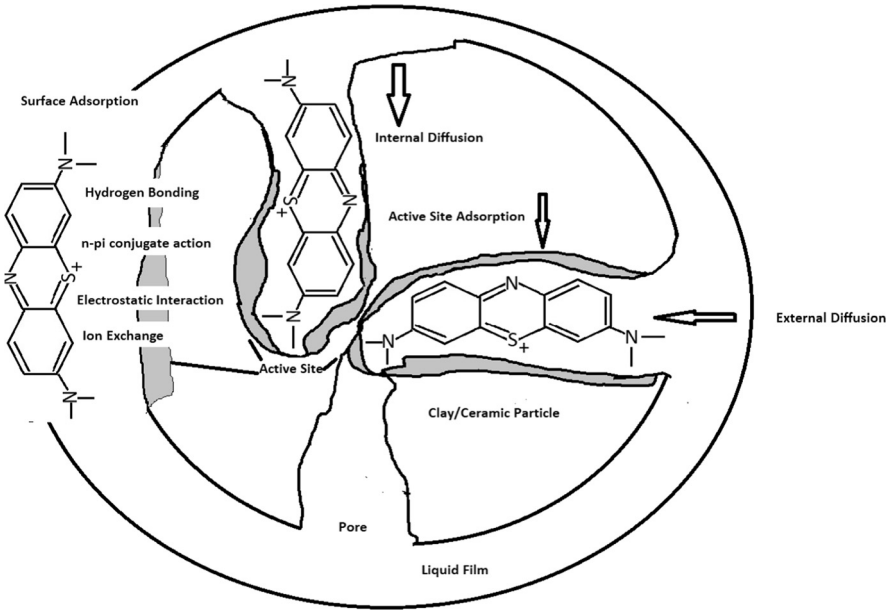

FIGURE 13.1 Graphical representation of the possible adsorption process of MB molecules on clay/ceramics.

13.3.9 A Possible Mechanism for Dye Adsorption

The interactions involved in the removal process this text discusses can be summarized diagrammatically in Figure 13.1.

13.4 CONCLUSION AND FUTURE SCOPE

This chapter presented a summary of methylene blue removal by various clay and ceramic-based adsorbents under different experimental conditions and their adsorption mechanism. It was observed that adsorption increases during the initial hours of reaction and then remains constant on achieving equilibrium with high methylene blue removal percentage. Most of the adsorbents showed the highest adsorption at a neutral pH, whereas some of the adsorbents work well in acidic and some in basic conditions, i.e. a range from 2–12.

An increase of MB concentration has resulted in higher uptake of MB molecules, whereas changes in adsorbent dose had a variable effect on MB removal capacity. In some experimental studies, an increase in adsorbent dose resulted in increased adsorption capacity due to increased surface area. In contrast, in some studies, it resulted in decreased or constant adsorption due to agglomeration. Adsorption experiments at different temperatures showed the process is endothermic nature in general. To describe the equilibrium studies of MB adsorption, the Langmuir and Freundlich models have been adopted in most studies. The pseudo-second-order kinetics very elegantly explained the kinetics of adsorption in most of the cases.

Development and modification of clay-based adsorbents and ceramic materials with high adsorption capacities and adsorption rate, which are minimally affected by variations of pH, temperature, MB concentration, presence of other inorganic and organic impurities, are some of the focus areas for future research.

REFERENCES

Adeyemo, AA, Adeoye, IO, & Bello, OS (2017). Adsorption of dyes using different types of clay: A review. *Applied Water Science*, *7*(2), 543–568.

Almeida, CAP, Debacher, NA, Downs, AJ, Cottet, L, & Mello, CAD (2009). Removal of methylene blue from colored effluents by adsorption on montmorillonite clay. *Journal of Colloid and Interface Science*, *332*(1), 46–53.

Arora, C, Soni, S, Sahu, S, Mittal, J, Kumar, P, & Bajpai, PK (2019). Iron based metal organic framework for efficient removal of methylene blue dye from industrial waste. *Journal of Molecular Liquids*, *284*, 343–352.

Auta, M, & Hameed, BH (2012). Modified mesoporous clay adsorbent for adsorption isotherm and kinetics of methylene blue. *Chemical Engineering Journal*, *198*, 219–227.

Auta, M, & Hameed, BH (2014). Chitosan–clay composite as highly effective and low-cost adsorbent for batch and fixed-bed adsorption of methylene blue. *Chemical Engineering Journal*, *237*, 352–361.

Basaleh, AA, Al-Malack, MH, & Saleh, TA (2019). Methylene Blue removal using polyamide-vermiculite nanocomposites: Kinetics, equilibrium and thermodynamic study. *Journal of Environmental Chemical Engineering*, *7*(3), 103107.

Bhatia, D, Sharma, NR, Singh, J, & Kanwar, RS (2017). Biological methods for textile dye removal from wastewater: A review. *Critical Reviews in Environmental Science and Technology*, *47*(19), 1836–1876.

Bleicher, RJ, Kloth, DD, Robinson, D, & Axelrod, P (2009). Inflammatory cutaneous adverse effects of methylene blue dye injection for lymphatic mapping/sentinel lymphadenectomy. *Journal of Surgical Oncology*, *99*(6), 356–360.

BouKhemakhem, A, & Rida, K (2017). Improvement adsorption capacity of methylene blue onto modified Tamazert kaolin. *Adsorption Science & Technology*, *35*(9–10), 753–773.

Chen, Xunjun. 2015. Modeling of Experimental Adsorption Isotherm Data. *Information*, *6*(1), 14–22. 10.3390/info6010014.

Dawood, S, & Sen, T (2014). Review on dye removal from its aqueous solution into alternative cost effective and non-conventional adsorbents. *Journal of Chemical and Process Engineering*, *1*(104), 1–11.

Doğan, M, & Alkan, M (2003). Adsorption kinetics of methyl violet onto perlite. *Chemosphere*, *50*(4), 517–528.

Duwal, N, Joshi, S, & Bhattarai, J (2016). Study on the removal of methylene blue by calcined-Kamerotar clays as an eco friendly low cost adsorbent. *Int J Adv Res Chem Sci*, *3*(11), 1–8.

El Mouzdahir, Y, Elmchaouri, A, Mahboub, R, Gil, A, & Korili, SA (2007). Adsorption of methylene blue from aqueous solutions on a Moroccan clay. *Journal of Chemical & Engineering Data*, *52*(5), 1621–1625.

Ghosh, D, & Bhattacharyya, KG (2002). Absorption of methylene blue on kaolinite. *Applied Clay Science*, *20*(6), 295–300.

Gurses, A, Dogar, Ç, Yalcın, M, Açıkyıldız, M, Bayrak, R, & Karaca, S (2006). The adsorption kinetics of the cationic dye, methylene blue, onto clay. *Journal of Hazardous Materials*, *131*(1–3), 217–228.

Hajjaji, M, Alami, A, & El Bouadili, A (2006). Removal of methylene blue from aqueous solution by fibrous clay minerals. *Journal of Hazardous Materials*, *135*(1–3), 188–192.

Harrou, A, Gharibi, E, Nasri, H, & El Ouahabi, M (2020). Thermodynamics and kinetics of the removal of methylene blue from aqueous solution by raw kaolin. *SN Applied Sciences*, *2*(2), 277.

Ho, YS, & Chiang, CC (2001). Sorption studies of acid dye by mixed sorbents. *Adsorption*, *7*(2), 139–147.

Jawad, AH, & Abdulhameed, AS (2020). Mesoporous Iraqi red kaolin clay as an efficient adsorbent for methylene blue dye: Adsorption kinetic, isotherm and mechanism study. *Surfaces and Interfaces*, *18*, 100422.

Kandisa, RV, Saibaba, KN, Shaik, KB, & Gopinath, R (2016). Dye removal by adsorption: A review. *Journal of Bioremediation and Biodegradation*, *7*(6).

Karaca, S, Gürses, A, Açışlı, Ö, Hassani, A, Kıranşan, M, & Yıkılmaz, K (2013). Modeling of adsorption isotherms and kinetics of Remazol Red RB adsorption from aqueous solution by modified clay. *Desalination and Water Treatment*, *51*(13−15), 2726–2739.

Khan, M (2020). Adsorption of methylene blue onto natural Saudi Red Clay: Isotherms, kinetics and thermodynamic studies. *Materials Research Express*, *7*(5), 5507.

Khenifi, A, Bouberka, Z, Sekrane, F, Kameche, M, & Derriche, Z (2007). Adsorption study of an industrial dye by an organic clay. *Adsorption*, *13*(2), 149–158.

Li, K, Zheng, Z, Huang, X, Zhao, G, Feng, J, & Zhang, J (2009). Equilibrium, kinetic and thermodynamic studies on the adsorption of 2-nitroaniline onto activated carbon prepared from cotton stalk fibre. *Journal of hazardous materials*, *166*(1), 213–220.

Mondal, S (2008). Methods of dye removal from dye house effluent—an overview. *Environmental Engineering Science*, *25*(3), 383–396.

Moussout, H, Ahlafi, H, Aazza, M, & Maghat, H (2018). Critical of linear and nonlinear equations of pseudo-first order and pseudo-second order kinetic models. *Karbala International Journal of Modern Science*, *4*(2), 244–254.

Nandi, BK, Goswami, A, & Purkait, MK (2009). Removal of cationic dyes from aqueous solutions by kaolin: Kinetic and equilibrium studies. *Applied Clay Science*, *42*(3–4), 583–590.

Njoya, D, Nsami, JN, Rahman, AN, LekeneNgouateu, RB, Hajjaji, M, & Nkoumbou, C (2017). Adsorption of Methylene Blue from Aqueous Solution onto Cordierite based ceramic. *Journal of Materials and Environmental Sciences*, *8*(5), 1803–1812.

Nnenna, NV, Philomena, KI, & Elijah, OC (2020). Removal of methylene blue dye from aqueous solution using modified Ngbo clay. *Journal of Materials Science Research and Reviews*, *5*(2), 33–46.

Noel, SD, & Rajan, MR (2015). Impact of dyeing industry effluent on ground water quality by water quality index and correlation analysis. *Research in Biotechnology*, *6*(1), 47–53.

Nyankson, E, Mensah, RQ, Kumafle, L, Gblerkpor, WN, Aboagye, SO, Asimeng, BO, & Tiburu, EK (2020). Dual application of natural clay material for decolorisation and adsorption of methylene blue dye. *Cogent Chemistry*, *6*(1), 1788291.

Özacar, M, & Şengil, İA (2006). A two-stage batch adsorber design for methylene blue removal to minimise contact time. *Journal of environmental management*, *80*(4), 372–379.

Ozdes, D, Duran, C, Senturk, HB, Avan, H, &Bicer, B (2014). Kinetics, thermodynamics, and equilibrium evaluation of adsorptive removal of methylene blue onto natural illitic clay mineral. *Desalination and Water Treatment*, *52*(1–3), 208–218.

Pandey, LM (2019). Enhanced adsorption capacity of designed bentonite and alginate beads for the effective removal of methylene blue. *Applied Clay Science*, *169*, 102–111.

Pawar, RR, Gupta, P, Sawant, SY, Shahmoradi, B, & Lee, SM (2018). Porous synthetic hectorite clay-alginate composite beads for effective adsorption of methylene blue dye from aqueous solution. *International Journal of Biological Macromolecules*, *114*, 1315–1324.

Rehman, MU, Manan, A, Uzair, M, Khan, AS, Ullah, A, Ahmad, AS, & Khan, MA (2021). Physicochemical characterisation of Pakistani clay for adsorption of methylene blue: Kinetic, isotherm and thermodynamic study. *Materials Chemistry and Physics*, *269*(2021), 124722.

Reisch, MS (1996). Asian textile dye makers are a growing power in a changing market. *Chemical & Engineering News*, *74*(3), 10–12.

Sahin, O, Kaya, M, & Saka, C (2015). Plasma-surface modification on bentonite clay to improve the performance of adsorption of methylene blue. *Applied Clay Science*, *116*, 46–53.

Saka, C, & Sahin, Ö (2011). Removal of methylene blue from aqueous solutions by using cold plasma-and formaldehyde-treated onion skins. *Coloration Technology*, *127*(4), 246–255.

Salh, DM, Aziz, BK, & Kaufhold, S (2020). High adsorption efficiency of Topkhana natural clay for methylene blue from medical laboratory wastewater: A linear and nonlinear regression. *Silicon*, *12*(1), 87–99.

Santos, SC, Oliveira, AF, & Boaventura, RA (2016). Bentonitic clay as adsorbent for the decolourisation of dyehouse effluents. *Journal of Cleaner Production*, *126*, 667–676.

Shahadat, M, & Isamil, S (2018). Regeneration performance of clay-based adsorbents for the removal of industrial dyes: A review. *RSC Advances*, *8*(43), 24571–24587.

Suteu, D, & Malutan, T (2013). Industrial cellolignin wastes as adsorbent for removal of methylene blue dye from aqueous solutions. *BioResources*, *8*(1), 427–446.

Vutskits, L, Briner, A, Klauser, P, Gascon, E, Dayer, AG, Kiss, JZ, & Morel, DR (2008). Adverse effects of methylene blue on the central nervous system. *Anesthesiology: The Journal of the American Society of Anesthesiologists*, *108*(4), 684–692.

Wang, J, & Guo, X (2020). Adsorption isotherm models: Classification, physical meaning, application and solving method. *Chemosphere*, *127279*.

Youcef, LD, Belaroui, LS, & López-Galindo, A (2019). Adsorption of a cationic methylene blue dye on an Algerian palygorskite. *Applied Clay Science*, *179*, 105145.